NASA TECHNICAL NOTE

NASA TN D-6305

C.1

NASA TN D-6305

FRACTURE OF THIN SECTIONS CONTAINING THROUGH AND PART-THROUGH CRACKS

by Thomas W. Orange, Timothy L. Sullivan, and Frederick D. Calfo

Lewis Research Center
Cleveland, Ohio 44135

NATIONAL AERONAUTICS AND SPACE ADMINISTRATION • WASHINGTON, D. C. • APRIL 1971

1. Report No. NASA TN D-6305	2. Government Accession No.	3. Recipient's Catalog No.
4. Title and Subtitle FRACTURE OF THIN SECTIONS CONTAINING THROUGH AND PART-THROUGH CRACKS		5. Report Date April 1971
		6. Performing Organization Code
7. Author(s) Thomas W. Orange, Timothy L. Sullivan, and Frederick D. Calfo		8. Performing Organization Report No. E-5657
9. Performing Organization Name and Address Lewis Research Center National Aeronautics and Space Administration Cleveland, Ohio 44135		10. Work Unit No. 124-08
		11. Contract or Grant No.
12. Sponsoring Agency Name and Address National Aeronautics and Space Administration Washington, D. C. 20546		13. Type of Report and Period Covered Technical Note
		14. Sponsoring Agency Code

15. Supplementary Notes

16. Abstract

Current fracture mechanics theory is used to illustrate the effects of crack dimensions and material properties on fracture stresses for through-thickness and part-through cracks. The implications of the analysis for leak-before-burst design of pressure vessels are discussed. The applicability of plane-strain theory to surface cracks in thin metal sections was studied experimentally. Aluminum and titanium alloy sheet specimens were tested at cryogenic temperatures. The specimens contained surface cracks of various lengths and depths or through cracks in the same range of cracks lengths. The fracture tests indicate that when Irwin's plastic zone size was less than about one-tenth of the uncracked ligament depth (thickness minus crack depth), surface-crack fracture behavior was in agreement with plane-strain theory. When the plastic zone was greater than the ligament depth, fracture stresses for surface-crack specimens were very nearly the same as for specimens with through-thickness cracks of the same original length.

17. Key Words (Suggested by Author(s)) Fracture mechanics; Fracture strength; Surface cracks; Aluminum alloys; Titanium alloys	18. Distribution Statement Unclassified - unlimited

19. Security Classif. (of this report)	20. Security Classif. (of this page)	21. No. of Pages	22. Price*
Unclassified	Unclassified	23	$3.00

*For sale by the National Technical Information Service, Springfield, Virginia 22151

FRACTURE OF THIN SECTIONS CONTAINING THROUGH AND PART-THROUGH CRACKS

by Thomas W. Orange, Timothy L. Sullivan, and Frederick D. Calfo

Lewis Research Center

SUMMARY

This report presents the results of an investigation of the applicability of plane-strain fracture mechanics theory to problems of surface cracks in thin metal sections. Fracture mechanics analysis is used to illustrate the effects of crack dimensions and material properties on fracture stress for through and part-through cracks. The currently accepted limits for the validity of the analysis are reviewed. Experimental results and the limitations they impose on the applicability of the analysis are discussed.

Included are the results of thin-sheet fracture tests of several materials at ambient and cryogenic temperatures. The materials and test temperatures are

1. Titanium-5Al-2.5 Sn ELI, 0.06- and 0.11-inch (1.6- and 2.9-mm) thick; -423° F (20 K)
2. Aluminum 2014-T6, 0.06-inch (1.6-mm) thick; -423° F (20 K)
3. Aluminum 2219-T87, 0.07-inch (1.7-mm) thick; 70°, -320°, and -423° F (300, 77, and 20 K)

Specimens containing semielliptical surface cracks of various lengths and depths and specimens containing through-thickness cracks in the same range of crack lengths were tested.

The fracture tests indicate that when Irwin's plastic zone size was less than about one-tenth of the uncracked ligament depth (thickness minus crack depth), surface-crack fracture behavior was in agreement with plane-strain theory. When the plastic zone was greater than the ligament depth, fracture stresses for surface-crack specimens were very nearly the same as for specimens with through-cracks of the same original length.

INTRODUCTION

Linear elastic fracture mechanics can be used with confidence only for a limited number of practical crack problems at the present time. Some of the uncertainties associated with through-crack testing are mentioned in reference 1 (authors' reply to discussion by R. H. Heyer). Irwin's surface-crack fracture analysis (ref. 2) assumes that conditions of plane strain prevail, and its application is customarily limited to crack depths of less than one-half the plate thickness. However, in spite of these apparently severe limitations, fracture mechanics theory is still useful. It can provide at least a qualitative description of the effects of material and geometrical parameters on fracture strength. In some cases, as will be shown later, it can also give a good quantitative description.

Current fracture mechanics analysis is based on linear elastic theory. In lieu of an elasto-plastic analysis, nonbrittle materials are treated in an approximate manner. Localized yielding at the tip of a crack is accounted for by adding a portion of the plastic zone length to the actual crack length. As long as the plastic zone is small compared to the crack length and specimen dimensions, this approximation has proven useful.

For small-scale yielding, the plastic zone size is proportional to the square of the ratio of stress intensity to yield strength. Thus, simple plastic zone corrections should be adequate as long as the crack length and specimen dimensions are greater than some multiple of this ratio squared. For edge-cracked or through-cracked specimens, the significant specimen dimensions are considered to be crack length, uncracked ligament length, and thickness. The proposed American Society for Testing and Materials (ASTM) plane-strain toughness test method (ref. 3) requires that thickness and crack length be greater than $2.5\left(K_{Ic}/\sigma_{ys}\right)^2$, and implies that the ligament length (width minus crack length) be greater than about $2\left(K_{Ic}/\sigma_{ys}\right)^2$. These criteria should be sufficiently conservative as to apply to all classes of materials. However, for some materials and/or test specimens (e.g., ref. 4) the theory appears applicable (within engineering accuracy) to much smaller cracks as well.

Irwin's analysis for a surface crack in a plate (ref. 2) assumes that plane-strain conditions prevail at fracture and that the crack dimensions are small compared with the plate dimensions. Brown and Srawley (ref. 1, pp. 30 to 33) indicate that the analysis may not be applicable if the crack depth is less than $2.5\left(K_{Ic}/\sigma_{ys}\right)^2$. Although the concept has not been adequately tested, there should probably be a minimum ligament depth (in this case, plate thickness minus crack depth) requirement also, as there is for the edge-cracked specimens. Thus, for two reasons (depth-to-thickness limit and minimum ligament depth), application of the analysis to material thicknesses much less than $5\left(K_{Ic}/\sigma_{ys}\right)^2$ cannot be assured.

The analysis of through cracks under mixed-mode failure conditions is also uncertain. It is well known that K_c decreases with increasing thickness until it reaches the limiting plane-strain value K_{Ic}. As discussed in reference 5 (pp. 138 to 143 and 155 to 158), K_c is not necessarily independent of crack length and specimen width. However, for many materials the form of the crack-extension resistance curve (R-curve) is such that, for sufficiently large test specimens, K_c is essentially constant (e.g., ref. 6). It is also possible to compute a nominal toughness parameter K_{cn} based on final load and original crack length (neglecting subcritical crack growth), but this is less likely to be constant. Although it is unsuitable for component design purposes, as shown by Kuhn (ref. 7), the concept of a constant K_{cn} is useful for the illustrative examples to follow.

The plastic zone at the crack tip is even less well understood than the subjects just discussed. Different analytical models lead to significantly different estimates of both the size and shape of the plastic zone. When used as corrections to a large crack length, these discrepancies will affect fracture toughness calculations only slightly. But uncertainty regarding the plastic zone size makes it very difficult to predict whether the plastic zone at the tip of a surface crack will extend completely through the plate thickness prior to failure. As is shown later, in the section Discussion of Results, this appears to significantly affect fracture behavior.

Rice has discussed various analytical models at length in reference 8. Hahn and Rosenfield (ref. 9) have compared observed plastic zones in Fe-3Si steel with several analytical models. They conclude that none of the models completely described the observed plastic zones, which were somewhat "butterfly-shaped." Lacking an exact description, a lower bound on the plastic zone size is still possible. The results of reference 9 suggest that the extent of the plastic zone (projected onto the crack plane) is roughly twice Irwin's plastic zone size term of reference 2, in the absence of large-scale yielding and nearby stress-free surfaces. Thus, if the uncracked ligament behind a surface crack is less than twice Irwin's plastic zone size, it is almost certain that the plastic zone has actually spread completely through the thickness. If the plastic zone at the tip of a crack is "butterfly-shaped," it might (under rising load) first reach the back surface at points out of the crack plane, as in figure 1 (taken from ref. 10).

In the present report, fracture mechanics analysis is used to predict the effects of crack dimensions and material properties on fracture stress for through cracks and part-through surface cracks. Fracture specimens with through cracks and with surface cracks were tested at cryogenic temperatures. The results are compared with the predicted trends.

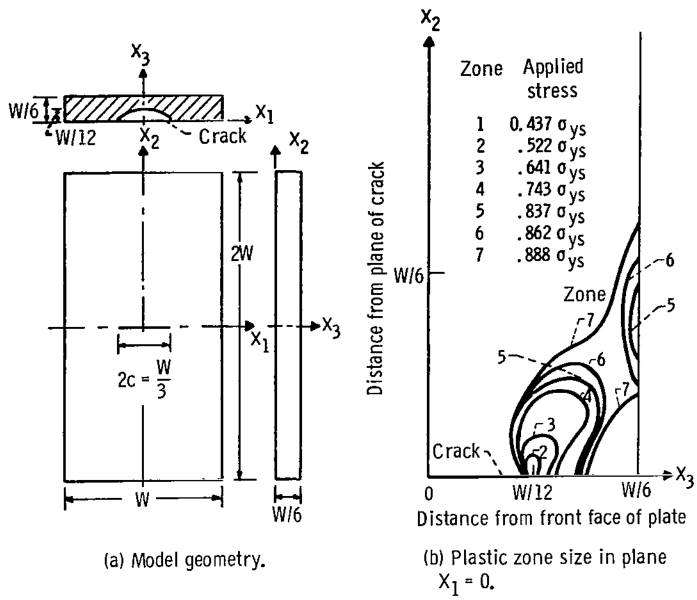

Figure 1. - Sample plastic zone. (From ref. 10.)

SYMBOLS

a	depth of semielliptical surface crack
c	half-length of through-crack or semielliptical surface crack
K_c	fracture toughness under mixed-mode fracture conditions
K_{cn}	nominal value of K_c, based on original crack length and final load
K_{Ic}	opening-mode (plane-strain) fracture toughness
K_Q	apparent value of K_{Ic}
M	free-surface correction factor (magnification factor)
t	plate thickness
W	specimen width
σ	fracture stress (based on gross area)
σ_{ys}	material yield strength (0.2 percent offset)
Φ	complete elliptical integral of second kind for argument $k^2 = 1 - (a/c)^2$

ANALYSIS

Even though its application to design problems is somewhat restricted, current fracture mechanics theory can be used to illustrate the effects of crack geometry and material properties on fracture strength and fracture behavior. For the sake of discussion, assume that through cracks are governed by plane-stress conditions and surface cracks by plane strain.

Effects of Crack Geometry

Fracture stresses for through-thickness cracks (from ref. 1) and for surface cracks (from ref. 2) in a wide flat plate can be written as

$$\sigma_{thru} = K_c \left[\frac{\pi}{2} 2c + \frac{1}{2}\left(\frac{K_c}{\sigma_{ys}}\right)^2\right]^{-1/2} \tag{1a}$$

$$\sigma_{surf} = K_{Ic} \frac{\Phi}{M} \left[\pi a + \frac{1}{4\sqrt{2}}\left(\frac{K_{Ic}}{\sigma_{ys}}\right)^2\right]^{-1/2} \tag{1b}$$

where Φ is a function of crack shape and M is a free-surface correction factor (taken by Irwin to be ~1.1 for crack depths less than one-half the thickness). The correction factor of Kobayashi and Moss (denoted as M_e in ref. 11) was used (rather than Irwin's) so that cracks deeper than one-half the thickness might be considered in this report. For the reader's convenience, a plot of M/Φ is included as figure 2.

For purposes of illustration, it is appropriate (as discussed by Irwin and Srawley in ref. 12) to consider the case where the thickness $t = K_c^2/2\pi\sigma_{ys}^2$. The previous equations can then be written (for this thickness only) as

$$\frac{\sigma_{thru}}{\sigma_{ys}} = \sqrt{2}\left(\frac{1}{2}\frac{2c}{t} + 1\right)^{-1/2} \tag{2a}$$

$$\frac{\sigma_{surf}}{\sigma_{ys}} = \sqrt{2}\,\frac{K_{Ic}}{K_c}\,\frac{\Phi}{M}\left[\frac{a}{t} + \frac{1}{2\sqrt{2}}\left(\frac{K_{Ic}}{K_c}\right)^2\right]^{-1/2} \tag{2b}$$

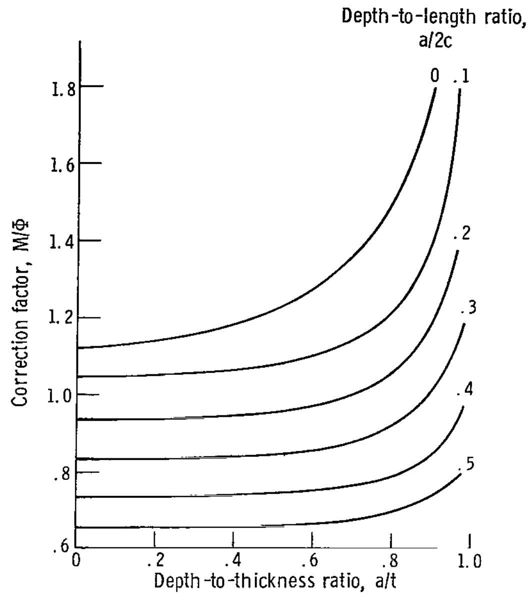

Figure 2. - Correction factor used in equation (2b).

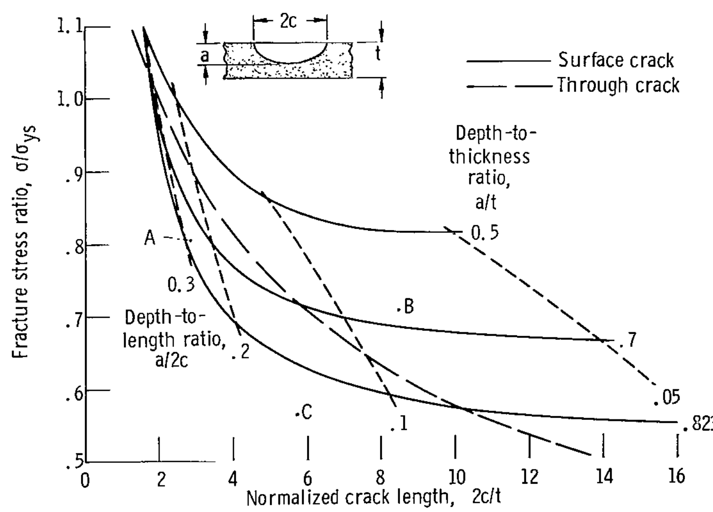

Figure 3. - Effect of crack geometry on predicted fracture stress for through and part-through cracks. Assumptions: $t = K_c^2/2\pi\sigma_{ys}^2$; $K_{Ic} = 0.5\,K_c$.

These equations are plotted in figure 3 for the case where $K_{Ic} = 0.5\ K_c$. Equation (2b) is plotted for constant crack shape a/2c as well as for constant depth a/t. The largest depth plotted is that for which the plastic zone is expected to just extend completely through the plate thickness at the onset of fracture. The applicability of the analysis to deeper cracks is highly questionable. If, as discussed earlier, the actual plastic zone size is taken to be twice Irwin's term, the limiting depth for this thickness is

$$\left(\frac{a}{t}\right)_{max} = 1 - \frac{1}{\sqrt{2}}\left(\frac{K_{Ic}}{K_c}\right)^2 \tag{3}$$

Figure 3 shows that theoretically a surface crack can fracture (or at least start to fracture) at a lower stress than a through-crack of the same length, and that this would be most likely to occur for a deep crack with a/2c about 0.2 to 0.3. With the aid of figure 3 we can speculate on the effect of crack geometry on the actual fracture process. Consider a surface crack whose geometry is defined by the point A. When the load is increased to $0.8\ \sigma_{ys}$, the crack should start to propagate rapidly through the thickness. Irwin (ref. 2) showed that crack extension should tend to produce a circular crack boundary, thus there should be little if any increase in crack length. The stress required to propagate a through-crack of the same length is much greater (about $0.9\ \sigma_{ys}$). Thus, the crack should self-arrest and become a stable through-thickness crack. If the crack were in a pressure vessel, the vessel would leak rather than fail catastrophically.

Consider now a surface crack whose geometry is defined by the point B. When the load is increased to $0.7\ \sigma_{ys}$, the crack should start to propagate through the thickness. But if there is no load relaxation, the applied stress will be more than sufficient to propagate a through crack of that length and the crack should continue to propagate. A pressure vessel with such a crack would probably fail catastrophically.

For the surface crack defined by point C, the plastic zone would surely grow through the thickness prior to failure, and most of the uncracked ligament would undergo plastic deformation. Under these conditions, fracture might well be controlled by the stress intensity at or near the major axis of the semiellipse. If this crack were in a pressure vessel, elastic theory cannot predict whether it would leak or burst. Lacking more powerful analytical methods, we might speculate that if the crack opening displacement were sufficiently large, the ligament might fail by tensile instability (and the vessel would leak), and that this would be most likely for long cracks. But the yielded ligament might also act as a plastic hinge, allowing the cracked region to bulge outward in the manner associated with through cracks (ref. 13). This would induce a bending stress which would further complicate the problem. Under these conditions it would be unwise to expect a cracked tensile specimen to simulate the behavior of a cracked pressure vessel.

The empirical relation developed by Eiber, Maxey, Duffey, and McClure of Battelle Memorial Institute (ref. 14, fig. 15), for part-through vee-notches in gas line pipe is quite similar in appearance to figure 3 of this report. Their burst tests also indicate that failure type (i.e., leak or burst) can be correlated with relative fracture stresses for through cracks and surface cracks of the same length. If fracture stress for a given surface crack is less than for a through crack of the same length, that surface crack will result in a leak at failure; if greater, catastrophic fracture will occur.

Effects of Material Properties

The limits of applicability of this analysis are also affected by the material properties. Equation (3) shows that the limiting crack depth (at which the plastic zone just penetrates the thickness) is also a function of the ratio K_{Ic}/K_c. Figure 4 shows the effect of K_{Ic}/K_c on fracture stress at the limiting depth (for this specific thickness). From this figure it appears that leak-before-burst failures cannot be predicted using elastic theory if K_{Ic} is greater than about 0.6 K_c (for this thickness). The lower the ratio K_{Ic}/K_c the wider the crack length range over which such failures can be predicted.

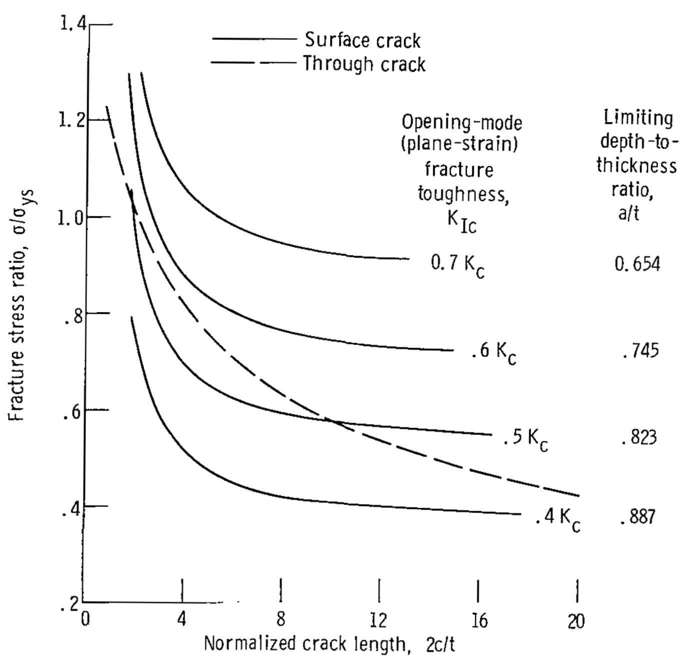

Figure 4. - Effect of material toughness on predicted fracture stress for through cracks and for part-through cracks at limiting depth. Assumption: $t = K_c^2/2\pi\sigma_{ys}^2$.

Interpretation of Experimental Data

Surface-crack fracture test data are often plotted as apparent K_{Ic} against initial crack depth. Judgment of the applicability of the plane-strain model is then based on the relative constancy of apparent K_{Ic} values over a range of crack sizes. However, such an approach can sometimes be misleading.

Surface cracks can propagate through the thickness on rising load and become through cracks prior to final fracture. In such a case, final fracture should be governed by crack length and the K_c value for the particular thickness, as in equation (1a). As suggested earlier, fracture might also be length dependent if the uncracked ligament undergoes gross plastic deformation. If final fracture is actually controlled by K_c and crack length but we unknowingly apply equation (1b), the apparent (but fictitious) toughness computed will be

$$(\text{Apparent } K_{Ic}) \cong K_c \frac{M}{\Phi} \sqrt{\frac{a}{c}} \tag{4}$$

Equation (4) is obtained by substituting fracture stress from equation (1a) into equation (1b) and neglecting plastic zone corrections for simplicity. It is plotted in figure 5 using the correction factor of figure 2.

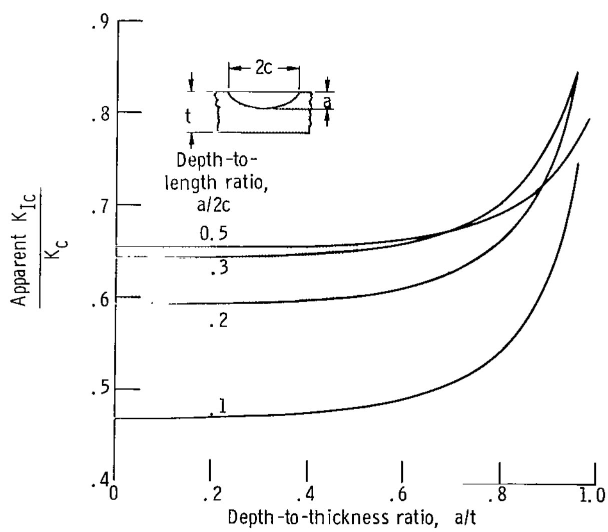

Figure 5. - Apparent surface-crack K_{Ic} when fracture is really controlled by K_c and crack length (elastic case).

Consider the crack geometry range $0.2 \le a/2c \le 0.5$ and $0 \le a/t \le 0.5$, which is shaded in figure 5 and which is a range of practical interest. It can be seen that, even if fracture is controlled by crack length (rather than depth), the apparent K_{Ic} varies only slightly (about ± 4 percent). From a series of tests in this range it might be concluded that since apparent K_{Ic} was approximately constant, fracture was controlled by crack depth.

For this reason, tests of specimens with through cracks (covering the same range of crack lengths) are desirable. The data can then be plotted as fracture stress against crack length. If the plane-strain, surface-crack model is appropriate, the plot should resemble figure 3 and the surface-crack data should be layered according to crack depth.

EXPERIMENTAL PROCEDURE

Materials

The titanium alloy was purchased in two thicknesses rolled from the same heat. Mill analyses for both are given in table I. The 2014-T6 aluminum alloy (unclad) was from the same lot as used in an earlier study (ref. 6). The analysis given was made by a commercial laboratory. The 2219-T87 aluminum alloy (also unclad) was from the same lot studied in reference 15, and its analysis is also given in table I.

The tensile properties listed in table II were determined by using the standard tensile specimen shown in figure 6(a) with differential-transformer extensometers.

Fracture Specimens

Titanium fracture specimen configurations were as shown in figures 6(b) and (c). All 2014-T6 specimens were as shown in figure 6(c). The 2219-T87 specimens were sized per figure 6(d) to be directly comparable with the surface-crack specimens tested in reference 15.

Natural cracks were grown from crack starters by low-stress fatigue cycling the specimens. Crack starters for all through-crack and most surface-crack specimens were made by electrical-discharge machining. For a few of the 2014-T6 surface-crack specimens, sharp surface grooves were machine scribed. All through-crack specimens and some surface-crack specimens were fatigue sharpened in tension. To obtain more elongated cracks, some surface cracks were extended in cyclic unidirectional bending. For all specimens, the nominal net cyclic stress was less than one-half the material yield strength.

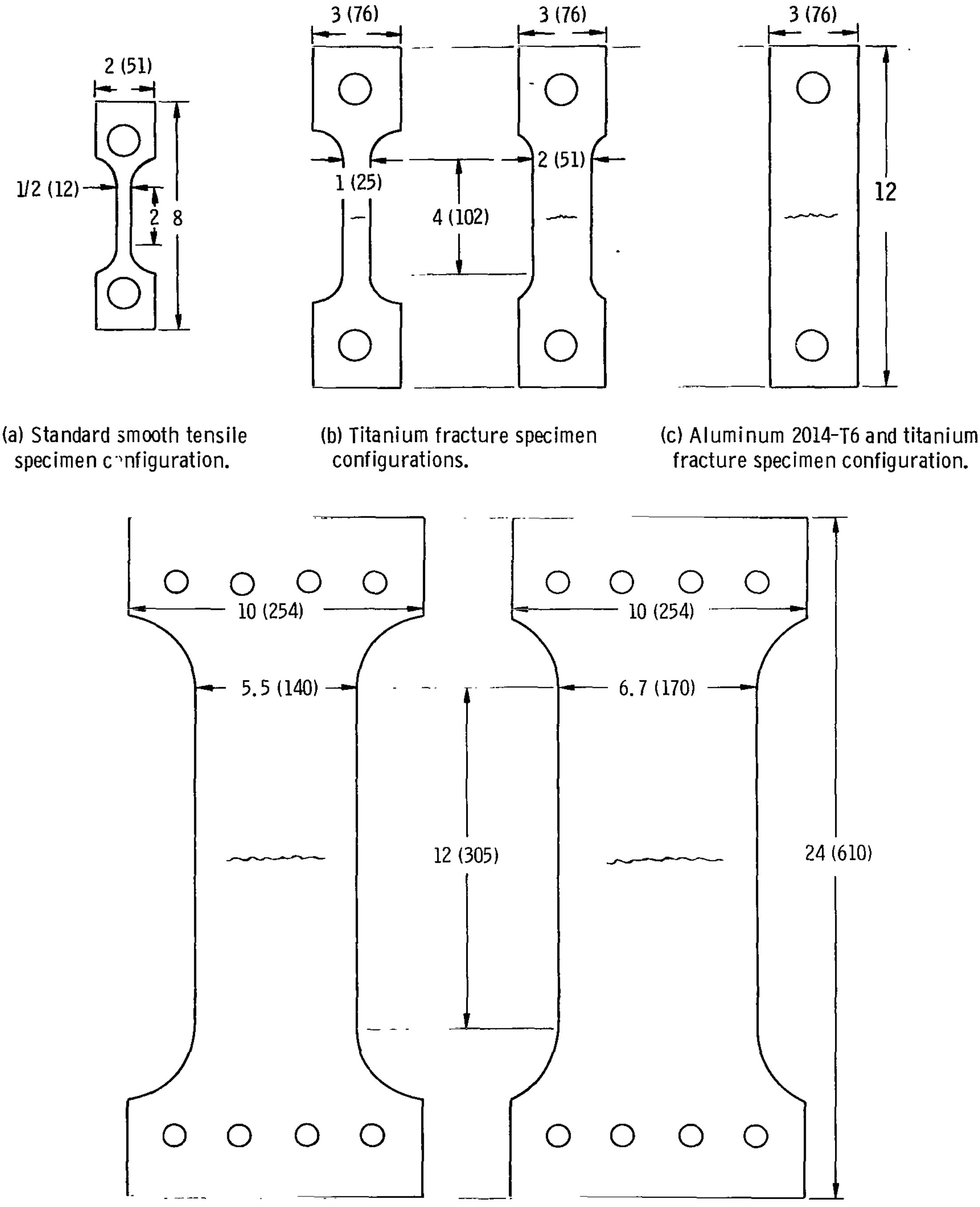

(a) Standard smooth tensile specimen configuration.

(b) Titanium fracture specimen configurations.

(c) Aluminum 2014-T6 and titanium fracture specimen configuration.

(d) Aluminum 2219-T87 fracture specimen configurations.

Figure 6. - Smooth tensile and fracture specimens. (Dimensions are in inches (mm).)

Apparatus and Procedure

The 2219-T87 through-crack fracture specimens were fitted with anti-buckling guides and tested in a 400 000-pound- (1.8-MN-) capacity screw-powered tensile testing machine. All other specimens were tested in hydraulic machines having capacities of 20 000, 24 000, and 120 000 pounds (89, 107, and 535 kN). For smooth tensile tests, differential-transformer extensometers were used to measure average strain over a 2-inch (5-cm) gage length. Cryogenic test temperatures were established by immersing the specimen in liquid nitrogen or in liquid hydrogen. A vacuum-jacketed cryostat with multilayer insulation was used to minimize boiloff. Cryogenic liquid level was maintained several inches above the upper specimen grip, and carbon resistors were used as level sensors.

RESULTS AND DISCUSSION

Nominal fracture toughness values for through-crack specimens were computed using the finite-width correction factor proposed by Feddersen (ref. 1, pp. 77 to 79). Equation (1a) can then be written

$$K_{cn} = \sigma\sqrt{W\theta \sec \theta}$$

where

$$\theta = \frac{\pi}{2}\left(\frac{2c}{W}\right) + \frac{1}{2W}\left(\frac{K_{cn}}{\sigma_{ys}}\right)^2 \tag{5}$$

Apparent fracture toughness K_Q values for surface-crack specimens were computed using equation (1b) (rearranged) and the free-surface correction factor of reference 11. Fracture test results and some calculated quantities are listed in tables III and IV.

Titanium Alloy

Figure 7 presents fracture stresses for through cracks and surface cracks in the thinner (0.06 in., 1.6 mm) titanium sheet at -423° F (20 K). The surface-crack tests are grouped according to depth-to-thickness ratio. The experimental trends are generally in good agreement with the predicted trends of figure 3. Nominal fracture toughness

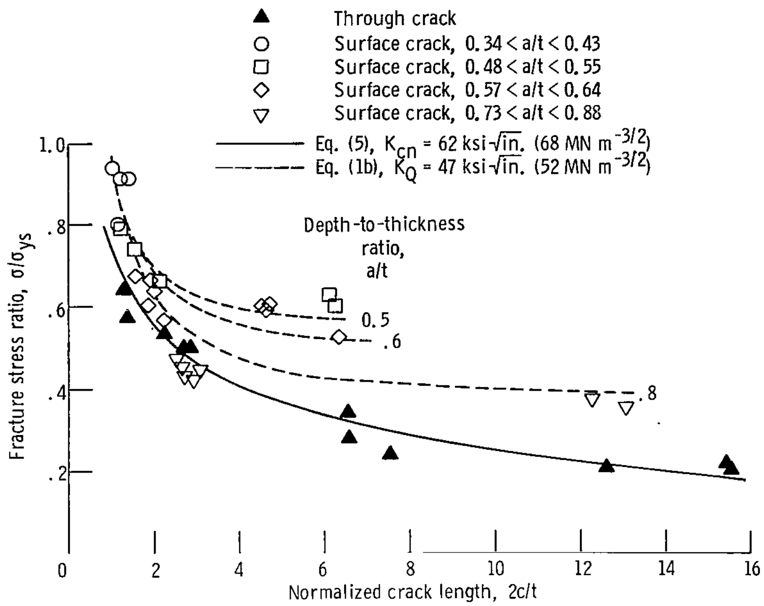

Figure 7. - Fracture stress for titanium-5Al-2.5 Sn ELI specimens 0.06-inch (1.6-mm) thick. Test temperature, -423° F (20 K); yield strength, 228.0 ksi (1570 MN/m^2).

K_{cn} for the through-crack specimens was essentially constant $\left(62 \text{ ksi}\sqrt{\text{in.}}\right.$ (68 MN m$^{-3/2}$), $\left.\text{average}\right)$. Apparent fracture toughness K_Q for the surface-crack tests was reasonably constant (47 ksi $\sqrt{\text{in.}}$ (52 MN m$^{-3/2}$), average) for all but the seven specimens with cracks deeper than 70 percent of the thickness. Note (fig. 7) that for the five of these specimens with short cracks (2c/t ~ 3), fracture stresses are within the scatter band for through-crack tests. Using the average K_Q value (47 ksi $\sqrt{\text{in.}}$), Irwin's plastic zone size is between 14 and 29 percent of the uncracked ligament depth for the seven deviant tests. However, as discussed earlier, this expression is probably a conservative (low) estimate of the actual plastic zone size, which may be several times larger.

Figure 8 presents fracture stresses for through cracks and surface cracks in the thicker (0.11-in., 2.9-mm) titanium sheet, also at -423° F (20 K). Here the surface-crack shapes were essentially constant (a/2c ~ 0.3) as crack depth was varied. Nominal fracture toughness K_{cn} for through-crack specimens was essentially constant (83 ksi $\sqrt{\text{in.}}$ (91 MN m$^{-3/2}$), average), as was apparent toughness K_Q for surface-crack specimens (59 ksi $\sqrt{\text{in.}}$ (65 MN m$^{-3/2}$), average). Fracture stresses for the three deepest surface-crack tests lie within or very near the scatter band for through-crack tests. For these three specimens, Irwin's plastic zone size (K_Q = 59 ksi $\sqrt{\text{in.}}$) is between 13 and 40 percent of the uncracked ligament depth.

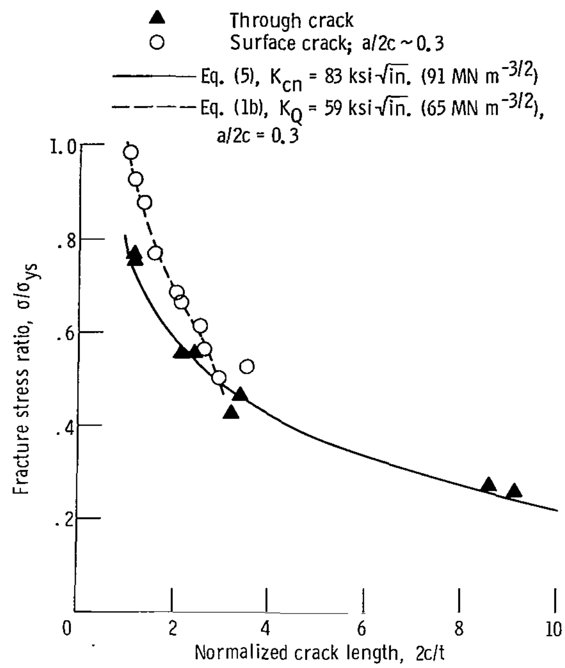

Figure 8. - Fracture stress for titanium-5Al-2.5 Sn ELI specimens 0.11-inch (2.9-mm) thick. Test temperature, -423° F (20 K); yield strength, 211 ksi (1450 MN/m^2).

Even though both thicknesses are from the same heat, the K_Q and K_{cn} average values are about 13 percent higher (and strengths are lower) for the thicker gage. However, the K_Q average values for both are within the range of K_{Ic} values reported in reference 16 for much thicker specimens.

Aluminum Alloys

Figure 9 presents fracture stresses for through cracks and surface cracks in 2014-T6 aluminum sheet (0.06-in. (1.6-mm) thick) at -423° F (20 K). Note that only for the shortest cracks is there any apparent difference between fracture stresses for through cracks and for surface cracks. Nominal fracture toughness K_{cn} was approximately constant (52 ksi $\sqrt{in.}$ (57 MN $m^{-3/2}$), average) for all but the two shortest through cracks. Apparent toughness K_Q was also constant (26 ksi $\sqrt{in.}$ (28 MN $m^{-3/2}$), average) for all but the four deepest surface cracks. For these four, Irwin's plastic zone size (based on 26 ksi $\sqrt{in.}$) was deeper than any uncracked ligament. For the eight other specimens, Irwin's plastic zone size was between 26 and 72 percent of the depth of the uncracked ligaments. However, even though constant, the K_Q values are unusually low. The surface-crack K_Q values reported in reference 17 for 2014-T62 alloy 0.5-inch (13-mm)

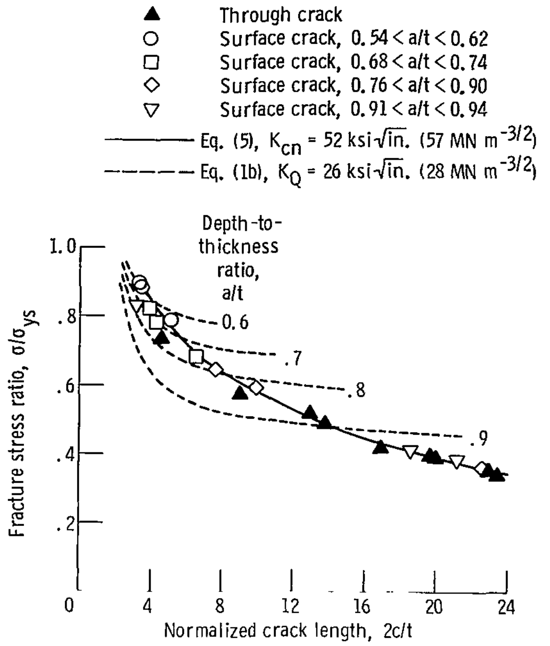

Figure 9. - Fracture stress for 2014-T6 aluminum specimens 0.06-inch (1.6-mm) thick. Test temperature, -423° F(20 K); yield strength, 80.3 ksi (554 MN/m²).

thick are nearly twice as large. If computed using reference 17 values for K_Q, Irwin's plastic zone would be deeper than any uncracked ligament. Analysis according to reference 11, where plastic zone size is related to fracture stress rather than to stress intensity, also indicates that the plastic zone did extend completely through the thickness prior to fracture for every test.

Figure 10 presents fracture stresses for through cracks and surface cracks in 2219-T87 aluminum sheet (0.07-in. (1.7-mm) thick) at ambient temperature, -320° F, and -423° F (300, 77, and 20 K). The surface-crack data are taken from reference 15; through-crack specimens from the same lot of material were tested at Lewis. Neither nominal toughness K_{cn} nor apparent toughness K_Q were constant at any temperature, and the curves of figure 10 were simply drawn through the through-crack data. Again there is little difference in fracture stresses for surface cracks and for through cracks of the same length. Based on the estimated K_{Ic} values of reference 15 (47 ksi $\sqrt{\text{in.}}$ at 70° F and 50 ksi $\sqrt{\text{in.}}$ at -320° and -423° F; 52 MN $m^{-3/2}$ at 300 K and 55 MN $m^{-3/2}$ at 77 and 20 K), the Irwin plastic zone sizes were greater than all uncracked ligaments. Thus, it is fairly certain that the surface-crack plastic zones penetrated the thickness prior to fracture in every test.

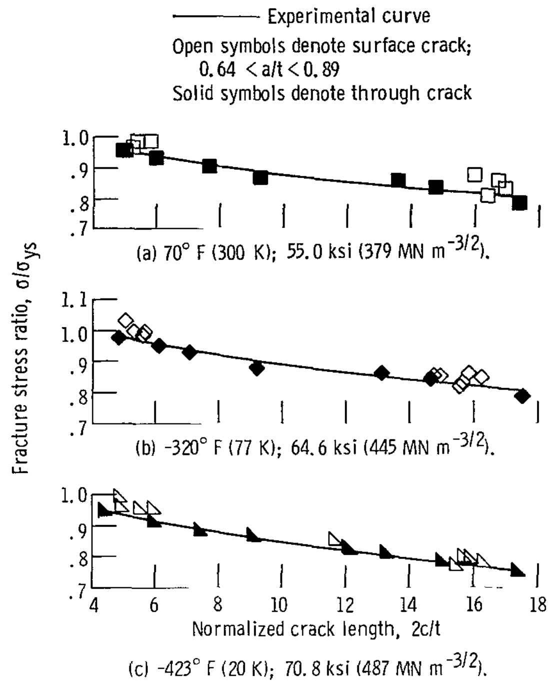

Figure 10. - Fracture stress for 2219-T87 aluminum specimens 0.07-inch (1.7-mm) thick for various test temperatures and yield strengths. (Surface crack data from ref. 15.)

Discussion of Results

The constant-K_{cn} concept is not sufficient to characterize through-crack fracture in the relatively tough 2219-T87 alloy. But for the less-tough titanium and 2014-T6 aluminum alloys, it relates fracture stress to original crack length quite well over the range of these tests.

The characterization of surface-crack fracture is not so straightforward. However, the results are consistent if they are classified according to the relative depths of the plastic zone and of the uncracked ligament. For most of the titanium specimens, where Irwin's plastic zone size was less than about 13 percent of the uncracked ligament depth, K_Q values were essentially constant and the plane-strain model (eq. (1b)) seems appropriate. For all the aluminum specimens, the plastic zone is believed to have extended completely through the thickness. Here fracture appears to be strongly related to crack length and the mixed-mode fracture toughness K_{cn}. The behavior of the remainder of the titanium specimens is harder to classify, but this may be due to the approximate nature of the plastic zone size term.

As discussed earlier, Irwin's surface-crack analysis should be usable if the actual plastic zone size is "small" with respect to the depth of the uncracked ligament. These tests suggest an approximate limit. If Irwin's plastic zone term is less than about one-tenth the depth of the uncracked ligament, the plane-strain model appears to be applicable even for thin sections. However, the parameter K_Q (which may or may not be equal to the plane-strain toughness K_{Ic}) must be carefully determined. When the plastic zone is greater than the depth of the uncracked ligament, final fracture usually appears to be related to crack length and mixed-mode fracture toughness.

The analysis and the preceding discussion assume that surface cracks do not propagate until rapid fracture occurs. However, some investigators have recently observed stable subcritical growth of surface cracks in some materials. Just prior to fracture, such a crack could be larger than its original dimensions but not yet through the thickness. In such a case, a K_Q value based on original crack depth and maximum load would be erroneously low. Subcritical growth might account for some (but not all) of the observed deviations of K_Q from a constant value.

SUMMARY OF RESULTS

The experiments reported herein indicate that the fracture behavior of thin sections containing surface cracks may be strongly influenced by the ratio of the crack-tip plastic zone size to the ligament depth (thickness minus crack depth). The experimental results can be summarized as follows:

1. When the Irwin plastic zone size at fracture was less than about one-tenth of the ligament depth, fracture behavior was in general as predicted by plane-strain theory.

2. When the plastic zone size was greater than the ligament depth, fracture stresses for surface-crack specimens were very nearly the same as for specimens with through cracks of the same original length. It should be recognized that these conclusions may not be applicable to other materials and/or thicknesses, and more definitive tests are required to either confirm or correct them.

Based on analysis using current fracture mechanics theory, as supported but limited by these tests, it can be postulated that:

1. Current fracture mechanics methods can be applied to leak-before-burst problems of thin-walled pressure vessels, but only if the plastic zone at failure is small with respect to the uncracked ligament. If so, leaks can be expected only for somewhat narrow ranges of crack geometry and material properties.

2. If the plastic zone is expected to penetrate the thickness prior to failure, current analytical methods cannot predict whether a vessel will leak or burst at fracture. Under these circumstances, a cracked tensile specimen may not adequately simulate a cracked pressure vessel.

Lewis Research Center,
National Aeronautics and Space Administration,
Cleveland, Ohio, January 7, 1971,
124-08.

REFERENCES

1. Brown, William F., Jr.; Srawley, John E.: Plane Strain Crack Toughness Testing of High Strength Metallic Materials. Spec. Tech. Publ. No. 410, ASTM, 1967.
2. Irwin, G. R.: Crack-Extension Force for a Part-Through Crack in a Plate. J. Appl. Mech., vol. 29, no. 4, Dec. 1962, pp. 651-654.
3. Anon: Tentative Method of Test for Plane-Strain Fracture Toughness of Metallic Materials. Designation E 399-70T. 1970 Book of ASTM Standards. Part 31. ASTM, July 1970, pp. 911-927.
4. Amateau, M. F.; and Steigerwald, E. A.: Test Methods for Determining Fracture Toughness of Metallic Materials. TRW Equipment Labs. (AFML-TR-67-145, AD-823594), Sept. 1967.
5. Srawley, John E.; and Brown, William F., Jr.: Fracture Toughness Testing Methods. Fracture Toughness Testing and its Applications. Spec. Tech. Publ. No. 381, ASTM, 1965, pp. 133-198. (Also available as NASA TN D-2599, 1965.)
6. Orange, Thomas W.: Fracture Toughness of Wide 2014-T6 Aluminum Sheet at -320° F. NASA TN D-4017, 1967.
7. Kuhn, P.: Strength Calculations for Sheet-Metal Parts with Cracks. Materials Res. Standards, vol. 8, no. 9, Sept. 1968, pp. 21-26.
8. Rice, J. R.: Mechanics of Crack Tip Deformation and Extension by Fatigue. Fatigue Crack Propagation. Spec. Tech. Publ. No. 415, ASTM, 1967, pp. 247-311.
9. Hahn, G. T.; and Rosenfield, A.: Plastic Flow in the Locale on Notches and Cracks in Fe-3Si Steel Under Conditions Approaching Plane Strain. Battelle Memorial Inst. (SSC-191, Ship Structure Committee, Dept. of the Navy, DDC No. AD-680123), Nov. 1968.

10. Ayres, David J.: A Numerical Procedure for Calculating Stress and Deformation Near a Slit in a Three-Dimensional Elastic-Plastic Solid. NASA TN D-4717, 1968.

11. Kobayashi, A. S.; and Moss, W. L.: Stress Intensity Magnification Factors for Surface-Flawed Tension Plate and Notched Round Tension Bar. Fracture; Proceedings of the Second International Conference on Fracture. Chapman and Hall Ltd., 1969, pp. 31-45.

12. Irwin, G. R.; and Srawley, J. E.: Progress in the Development of Crack Toughness Fracture Tests. Materialpruefung, vol. 4, no. 1, Jan. 20, 1962, pp. 1-11.

13. Anderson, Robert B.; and Sullivan, Timothy L.: Fracture Mechanics of Through-Cracked Cylindrical Pressure Vessels. NASA TN D-3252, 1966.

14. Eiber, R. J.; Maxey, W. A.; Duffy, A. R.; and McClure, G. M.: Behavior of Through-Wall and Surface Flaws in Cylindrical Vessels. Presented at the National Symposium on Fracture Mechanics. Lehigh Univ., Bethlehem, Pa., June 1968.

15. Masters, J. N.; Haese, W. P.; and Finger, R. W.: Investigation of Deep Flaws in Thin Walled Tanks. Boeing Co. (NASA CR-72606), Dec. 1969.

16. Pyle, Richard; Schillinger, David E.; and Carman, Carl M.: Plane Strain, Fracture Toughness and Mechanical Properties of 2219-T87 Aluminum and 5A1-2.5 Sn ELI Titanium Alloy Weldments and One Inch Thick 5A1-2.5Sn ELI Titanium Alloy Plate. Rep. FA-R-1897, Frankford Arsenal (NASA CR-72154), Sept. 1968.

17. Hall, L. R.: Plane-Strain Cyclic Flaw Growth in 2014-T62 Aluminum and 6Al-4V (ELI) Titanium. Rep. D2-114465-1, Boeing Co. (NASA CR-72396), Nov. 1968.

TABLE I. - CHEMICAL COMPOSITION OF MATERIALS TESTED

[Composition in percent by weight.]

Alloy	Al	C	Cr	Cu	Fe	H	Mg	Mn	N	O	Si	Sn	Ti	V	Zn	Zr
Ti-5Al-2.5 Sn (0.06 in., 1.6 mm)	5.3	0.02	----	----	0.18	0.0040	-----	0.01	0.007	0.098	----	2.5	Bal.	----	----	----
Ti-5Al-2.5 Sn (0.11 in., 2.9 mm)	5.3	.02	----	----	.18	.0034	-----	.01	.007	.091	----	2.5	Bal.	----	----	----
Aluminum 2014-T6	Bal.	----	0.04	4.45	.60	.0005	0.57	.69	.0012	.0005	0.92	---	0.02	----	0.05	----
Aluminum 2219-T87	Bal.	----	----	5.85	.19	------	.012	.25	------	------	.12	---	.09	0.08	.09	0.11

TABLE II. - TENSILE PROPERTIES OF TEST MATERIALS

[Average; longitudinal direction.]

Alloy	Test temperature		Yield strength		Ultimate strength		Elastic modulus		Elongation in 2 in. (5 cm), percent
	^{o}F	K	ksi	M/Nm^2	ksi	MN/m^2	psi	N/m^2	
Ti-5Al-2.5 Sn (0.06 in., 1.6 mm)	70	300	119	821	129	887	17×10^6	120×10^9	14
	-320	77	193	1330	202	1390	19	130	16
	-423	20	228	1570	247	1710	19	130	13
Ti-5Al-2.5 (0.11 in., 2.9 mm)	70	300	105	727	114	785	17×10^6	120×10^9	18
	-320	77	178	1230	189	1300	19	130	19
	-423	20	211	1450	223	1540	(a)	(a)	(a)
Aluminum 2014-T6	70	300	65.0	448	72.3	499	10×10^6	72×10^9	(b)
	-320	77	75.2	519	86.7	598	12	79	(b)
	-423	20	80.3	554	99.7	687	12	80	(b)
Aluminum 2219-T87	70	300	55.0	379	67.7	467	11×10^6	74×10^9	11
	-320	77	64.5	445	84.0	579	11	79	12
	-423	20	70.7	487	96.3	664	12	83	14

[a] Measurement considered unreliable.

[b] Not measured.

TABLE III. - THROUGH-CRACK FRACTURE TEST DATA

Alloy	Test temperature		Specimen width, W		Specimen thickness, t		Initial crack length, 2c		Gross fracture stress, σ		Nominal fracture toughness, K_{cn}	
	°F	K	in.	mm	in.	mm	in.	mm	ksi	MN/m^2	ksi $\sqrt{in.}$	MN $m^{-3/2}$
Ti-5Al-2 Sn (0.06 in., 1.6 mm)	-423	20	2.00	51	0.0624	1.58	0.080	2.0	147.1	1010	58.7	64.5
			1.00	25	.0616	1.56	.085	2.2	131.1	904	52.8	58.0
			2.00	51	.0632	1.61	.141	3.6	123.0	848	62.9	69.1
			1.00	25	.0639	1.62	.172	4.4	115.5	796	66.2	72.7
			2.00	51	.0632	1.61	.179	4.5	115.1	794	65.8	72.3
			1.00	25	.0629	1.60	.414	10.5	63.9	441	60.1	66.0
			2.00	51	.0640	1.63	.420	10.7	78.3	540	67.8	74.5
			1.00	25	.0640	1.63	.481	12.2	54.6	376	57.7	63.4
			2.00	51	.0628	1.60	.793	20.1	46.8	323	59.1	64.9
			3.00	76	.0640	1.63	.988	25.1	48.5	334	66.0	72.5
			3.00	76	.0639	1.62	.995	25.3	44.9	310	61.2	67.2
Ti-5Al-2.5 Sn (0.11 in., 2.9 mm)	-423	20	1.00	25	0.1115	2.83	0.123	3.1	161.3	1110	86.7	95.3
			2.00	51	.1122	2.85	.129	3.3	158.3	1090	84.6	93.0
			1.00	25	.1126	2.86	.240	6.1	116.9	806	83.1	91.3
			2.00	51	.1135	2.88	.269	6.8	119.0	821	86.0	94.5
			1.00	25	.1128	2.87	.360	9.1	90.3	623	80.4	88.3
			2.00	51	.1128	2.87	.381	9.7	97.3	671	82.3	90.4
			3.00	76	.1162	2.95	.994	25.2	58.3	402	80.5	88.5
			3.00	76	.1157	2.94	1.051	26.7	55.2	381	79.1	86.9
Aluminum 2014-T6	-423	20	3.00	76	0.0613	1.56	0.277	7.0	59.3	409	46.5	51.1
					.0622	1.58	.278	7.1	58.8	405	46.0	50.5
					.0617	1.57	.557	14.1	46.5	321	49.6	54.5
					.0600	1.52	.775	19.7	41.9	289	53.3	58.6
					.0613	1.56	.846	21.5	39.5	272	52.6	57.8
					.0611	1.55	1.032	26.2	34.2	236	50.9	55.9
					.0604	1.53	1.187	30.1	32.2	222	53.0	58.2
					.0602	1.53	1.204	30.6	31.5	217	52.2	57.4
					.0608	1.54	1.399	35.5	28.4	196	53.0	58.2
					.0611	1.55	1.432	36.4	27.5	190	52.2	57.4
Aluminum 2219-T87	70	300	5.5	140	0.0676	1.72	0.334	8.5	52.5	362	53.1	58.3
					.0672	1.71	.402	10.2	51.3	354	56.1	61.6
					.0673	1.71	.515	13.1	49.8	343	60.8	66.8
					.0676	1.72	.623	15.8	47.9	330	63.2	69.4
			6.7	170	0.0670	1.70	0.909	23.1	47.3	326	76.0	83.5
					.0680	1.73	1.004	25.5	46.1	318	77.1	84.7
					.0682	1.73	1.186	30.1	43.4	299	77.5	85.2
	-320	77	5.5	140	0.0685	1.74	0.332	8.4	63.2	436	64.9	71.3
					.0687	1.74	.420	10.7	61.5	424	69.6	76.5
					.0680	1.73	.480	12.2	60.2	415	72.1	79.2
					.0676	1.72	.621	15.8	57.1	394	75.5	83.0
			6.7	170	0.0673	1.71	0.884	22.5	55.9	385	88.1	96.8
					.0683	1.73	.998	25.3	54.6	376	90.9	99.9
					.0686	1.74	1.203	30.6	51.1	352	91.7	100.8
	-423	20	5.5	140	0.0682	1.73	0.297	7.5	66.7	460	61.3	67.4
					.0680	1.73	.400	10.2	64.6	445	67.7	74.4
					.0672	1.71	.492	12.5	62.6	432	71.5	78.6
					.0675	1.71	.610	15.5	61.5	424	78.2	85.9
			6.7	170	0.0683	1.73	0.825	21.0	58.2	401	83.9	92.2
					.0676	1.72	.891	22.6	57.5	396	85.9	94.4
					.0686	1.74	1.027	26.1	55.7	384	88.9	97.7
					.0684	1.74	1.184	30.1	53.6	370	91.4	100.4

TABLE IV. - SURFACE-CRACK FRACTURE TEST DATA

Alloy	Test temperature		Specimen width, W		Specimen thickness, t		Crack depth, a		Crack length, 2c		Gross fracture stress, σ		Apparent fracture toughness, K_Q	
	^oF	K	in.	mm	in.	mm	in.	mm	in.	mm	ksi	MN/m^2	ksi $\sqrt{in.}$	MN $m^{-3/2}$
Ti-5A1-2.5 Sn (0.06 in., 1.6 mm)	-423	20	1.00	25	0.0630	1.60	0.022	0.56	0.089	2.26	207.6	1430	51.8	56.9
			1.00	25	.0628	1.60	.024	.61	.078	1.98	207.5	1430	49.8	54.7
			1.00	25	.0631	1.60	.027	.69	.065	1.65	213.3	1470	47.1	51.8
			2.00	51	.0635	1.61	.027	.69	.075	1.91	182.7	1260	42.8	47.0
			1.00	25	.0636	1.62	.031	.79	.077	1.96	180.8	1250	43.1	47.4
			2.00	51	.0643	1.63	.033	.84	.099	2.51	169.0	1170	45.4	49.9
			2.00	51	.0621	1.58	.034	.86	.132	3.35	152.3	1050	46.0	50.5
			1.00	25	.0648	1.65	.037	.94	.102	2.59	153.5	1060	42.0	46.1
			2.00	51	.0635	1.61	.038	.97	.122	3.10	152.0	1050	45.3	49.8
			1.00	25	.0647	1.64	.040	1.02	.123	3.12	137.9	951	41.3	45.4
			2.00	51	.0641	1.63	.040	1.02	.128	3.25	145.7	1000	44.6	49.0
			1.00	25	.0650	1.65	.041	1.04	.147	3.73	130.0	896	42.1	46.3
			2.00	51	.0628	1.60	.046	1.17	.158	4.01	107.4	741	37.1	40.8
			1.00	25	.0640	1.63	.050	1.27	.173	4.39	102.4	706	37.9	41.6
			2.00	51	.0646	1.64	.051	1.30	.175	4.45	98.0	676	36.6	40.2
			2.00	51	.0646	1.64	.056	1.42	.190	4.83	96.7	667	40.2	44.2
			1.00	25	.0642	1.63	.056	1.42	.200	5.08	101.5	700	43.8	48.1
			2.00	51	.0631	1.60	.031	.79	.297	7.54	138.3	954	48.2	53.0
			1.00	25	.0630	1.60	.033	.84	.286	7.26	136.9	944	48.8	53.6
			1.00	25	.0639	1.62	.033	.84	.300	7.62	136.9	944	49.0	53.8
			1.00	25	.0640	1.63	.034	.86	.391	9.93	143.6	990	54.2	59.6
			2.00	51	.0637	1.62	.035	.89	.399	10.13	138.0	952	52.9	58.1
			1.00	25	.0622	1.58	.037	.94	.393	9.98	120.4	830	47.3	52.0
			2.00	51	.0639	1.62	.043	1.09	.590	14.99	111.7	770	50.0	54.9
					.0633	1.61	.045	1.14	.351	8.92	106.1	732	45.6	50.1
					.0638	1.62	.048	1.22	.782	19.86	85.1	587	42.4	46.6
					.0627	1.59	.049	1.24	.820	20.83	80.6	556	41.4	45.6
Ti-5A1-2.5 Sn (0.11 in., 2.9 mm)	-423	20	1.00	25	0.1157	2.94	0.023	0.58	0.118	3.00	207.6	1430	56.9	62.5
			2.00	51	.1122	2.85	.037	.94	.129	3.28	195.5	1350	59.8	65.7
			1.00	25	.1133	2.88	.043	1.09	.153	3.89	184.9	1270	61.3	67.4
			1.00	25	.1129	2.87	.056	1.42	.179	4.55	162.1	1120	58.4	64.2
			1.00	25	.1128	2.87	.068	1.73	.227	5.77	144.0	993	58.6	64.4
			2.00	51	.1147	2.91	.073	1.85	.247	6.27	139.9	965	59.6	65.5
			1.00	25	.1111	2.82	.077	1.96	.290	7.37	118.9	820	54.8	60.2
			2.00	51	.1143	2.90	.084	2.13	.291	7.39	129.0	889	61.2	67.2
			1.00	25	.1161	2.95	.097	2.46	.342	8.69	105.4	727	57.1	62.7
			2.00	51	.1119	2.84	.101	2.57	.337	8.56	110.4	761	65.3	71.8
Aluminum 2014-T6	-423	20	3.00	76	0.0622	1.58	0.034	0.86	0.206	5.23	72.1	497	25.7	28.2
			2.99		.0620	1.57	.035	.89	.213	5.41	70.8	488	25.6	28.1
			2.99		.0615	1.56	.038	.97	.311	7.90	63.4	437	25.4	27.9
			2.99		.0615	1.56	.042	1.07	.403	10.24	55.1	380	24.1	26.5
			3.01		.0600	1.52	.044	1.12	.232	5.89	66.2	456	27.4	30.1
			3.00		.0613	1.56	.044	1.12	.265	6.73	63.1	435	26.8	29.4
			2.99		.0605	1.54	.046	1.17	.457	11.61	51.7	356	24.7	27.1
			2.99		.0612	1.55	.051	1.30	.609	15.47	47.8	330	26.6	29.2
			3.00		.0603	1.53	.054	1.37	1.275	32.39	31.4	217	21.5	23.6
			3.01		.0600	1.52	.055	1.40	1.115	28.32	33.6	232	24.9	27.4
			3.00		.0603	1.53	.055	1.40	1.363	34.62	29.6	204	21.7	23.8
			3.00		.0619	1.57	.058	1.47	.198	5.03	66.7	460	34.2	37.6

NASA-Langley, 1971 —— 32 E-5657

NATIONAL AERONAUTICS AND SPACE ADMINISTRATION
WASHINGTON, D.C. 20546

OFFICIAL BUSINESS
PENALTY FOR PRIVATE USE $300

FIRST CLASS MAIL

POSTAGE AND FEES PAID
NATIONAL AERONAUTICS AND
SPACE ADMINISTRATION

06U 001 42 51 3CS 71.10 00903
AIR FORCE WEAPONS LABORATORY /WLOL/
KIRTLAND AFB, NEW MEXICO 87117

ATT E. LOU BOWMAN, CHIEF,TECH. LIBRARY

POSTMASTER: If Undeliverable (Section 158 Postal Manual) Do Not Return

"The aeronautical and space activities of the United States shall be conducted so as to contribute . . . to the expansion of human knowledge of phenomena in the atmosphere and space. The Administration shall provide for the widest practicable and appropriate dissemination of information concerning its activities and the results thereof."

—NATIONAL AERONAUTICS AND SPACE ACT OF 1958

NASA SCIENTIFIC AND TECHNICAL PUBLICATIONS

TECHNICAL REPORTS: Scientific and technical information considered important, complete, and a lasting contribution to existing knowledge.

TECHNICAL NOTES: Information less broad in scope but nevertheless of importance as a contribution to existing knowledge.

TECHNICAL MEMORANDUMS: Information receiving limited distribution because of preliminary data, security classification, or other reasons.

CONTRACTOR REPORTS: Scientific and technical information generated under a NASA contract or grant and considered an important contribution to existing knowledge.

TECHNICAL TRANSLATIONS: Information published in a foreign language considered to merit NASA distribution in English.

SPECIAL PUBLICATIONS: Information derived from or of value to NASA activities. Publications include conference proceedings, monographs, data compilations, handbooks, sourcebooks, and special bibliographies.

TECHNOLOGY UTILIZATION PUBLICATIONS: Information on technology used by NASA that may be of particular interest in commercial and other non-aerospace applications. Publications include Tech Briefs, Technology Utilization Reports and Technology Surveys.

Details on the availability of these publications may be obtained from:

SCIENTIFIC AND TECHNICAL INFORMATION OFFICE

NATIONAL AERONAUTICS AND SPACE ADMINISTRATION

Washington, D.C. 20546